



Short-term seismicity patterns along the most active faults in Iran

Majid Nemati¹ · Reza Derakhshani^{2,3}

Received: 16 December 2017 / Accepted: 21 July 2020 / Published online: 5 August 2020
© Universidad Complutense de Madrid 2020

Abstract

In this study, six seismically active fault systems located in different tectonic regimes have been surveyed. The data were from three Persian seismotectonic provinces (Alborz-Azarbaijan, Zagros and East-Central Iran) with different seismic properties, covering a time span of 8 years. The earthquake (Eq.) data have been recorded by the seismological network of the Institute of Geophysics of the University of Tehran, Iran (IGUT), the International Institute of Earthquake Engineering and Seismology of Iran (IIEES), and also include the early large instrumental earthquakes in the Engdahl catalog. During this period, few months of seismic quiescence occurred on the entire length of both Dasht-e Bayaz (DB) and Abiz faults, while most of the moderate and large earthquakes occurred after few months of lack of seismicity on the Main Recent fault, DB, Golbaf and Kazeroun faults. Moreover, single and triple migration patterns of seismicity were regularly seen along Golbaf fault and North Tabriz fault (NTF), respectively. Some large earthquakes (the 2011, M_N 5.2 Eq. of Golbaf F. and the 2008, M_N 5.2 Eq. of NTF) occurred at the end of these seismicity migration patterns. Along NTF, a diffuse seismicity with no specific seismic pattern has been distinguished. In all the case studies and during the investigated time period the entire lengths of the fault systems were not active at the same time. Finally, there is not a clear relationship between the duration of the seismic gaps and the magnitude of large earthquakes with different co-seismic rupture lengths in depth.

Keywords Earthquake · Seismicity · Pattern · Quiescence · Migration · Fault · Iran

Resumen

En el presente trabajo se estudian seis sistemas de fallas activas sísmicamente localizados en diferentes contextos tectónicos. Los datos han sido obtenidos de tres provincias sismotectónicas persas (Alborz-Azarbaijan, Zagros y Centro-Este de Iran) con diferentes propiedades sísmicas y seguidos durante 8 años. Los datos de terremotos (Eq) han sido registrados mediante una red sismológica en el Instituto de Geofísica de la Universidad de Teheran, Irán (IGUT), el Instituto Internacional de Ingeniería y Sismología de Irán (IIEES), incluyendo también una gran cantidad de datos obtenidos del catálogo Engdahl. Durante este periodo hubo pocos meses de estabilidad a lo largo de las fallas de Dasht-e Bayaz (DB) y Abiz, mientras que la mayoría de los terremotos moderados y de importancia aparecieron después de uno pocos meses de ausencia de sismicidad en las fallas recientes más importantes (DB) Golbaf y Kazeroum. Las tendencias de migración individual y triple fueron comúnmente las más observadas a lo largo de las fallas de Golbaf y del Norte de Tabriz (NTF) respectivamente. Algunos terremotos de gran intensidad (el de 2011, M_N 5.2 Eq. of Golbaf F., y el de 2008, M_N 5.2 Eq. of NTF) sucedieron al final de estas tendencias de migración sísmicas. Se ha distinguido una sismicidad difusa, sin una tendencia clara, a lo largo de NTF. Las fallas no fueron activas al mismo en los diferentes puntos de estudio durante el periodo de observación. Finalmente, no

✉ Majid Nemati
nematimajid_1974@uk.ac.ir

¹ Department of Geology, Faculty of Science and Earthquake Research Center of Shahid, Bahonar University of Kerman, Pajouhesh Sq., Kerman, Iran

² Department of Geology, Faculty of Science of Shahid, Bahonar University of Kerman, Pajouhesh Sq., Kerman, Iran

³ Department of Earth Sciences, Utrecht University, Utrecht, The Netherlands

hay una relación clara entre la duración de los periodos de ausencia de sismicidad y la magnitud de los principales terremotos que tienen diferente ruptura de co-sismicidad en longitud y profundidad.

Palabras clave Terremoto · Sismicidad · Patrón · Inactividad · Migración · Falla · Irán

1 Introduction

To address the issue of earthquake potential assessment along active faults, which is rather a difficult and challenging research topic in seismology, it is necessary to look at a roughly complete seismic and geodetic dataset; for example, GPS studies, analysis of the seismic moment accumulation rates on faults, systematic analysis of historical earthquake records and also trenching and isotopic dating of faults. These last items can reveal the history of seismic moment releases in the past and the slip history of past earthquakes. Moreover, investigation of seismicity pattern on space–time diagrams along active faults could necessarily be assumed as one of the important supplementary materials for the assessment of the potential of earthquake occurrence. Considering the importance of the seismic gaps along the fault segments, monitoring the active faults could lead us to lose the damages of the earthquakes. Indeed, a multi-disciplinary analysis of the information about the kind of the above mentioned studies will give us a chance to gain a meaningful assessment of potential of earthquake occurrence on faults.

Seismicity pattern is the most reported precursory phenomenon in short-term and intermediate-term as well as long-term precursors range (e.g. Scholz 1990). Space–time diagram of earthquakes along an active fault is one of the highly informative way to find any seismicity patterns, including seismic quiescence (an area without seismicity) before large earthquakes, aftershocks elongation and also migration of the seismicity (e.g. Lay et al. 1982; Scholz 1988; Berberian et al. 2001; Campos et al. 2002; Gheitanchi and Raeissi 2004; Berberian 2005). Moreover, characteristic patterns on spatial and temporal distribution of the seismicity help us to find seismic cycles along the active faults (e.g. Mogi 1977, 1962). Lay et al. (1982) investigated the space–time diagrams of major earthquakes in the Circum-Pacific Belt. They found the rupture characteristics of large shallow earthquakes, used for the classification of the earthquakes in different categories, by applying the asperity model to explain the earthquake processes.

The space–time diagrams of the seismicity along a specific fault strike could illustrate foreshock and aftershock sequences, approximate rupture length, and an estimation of

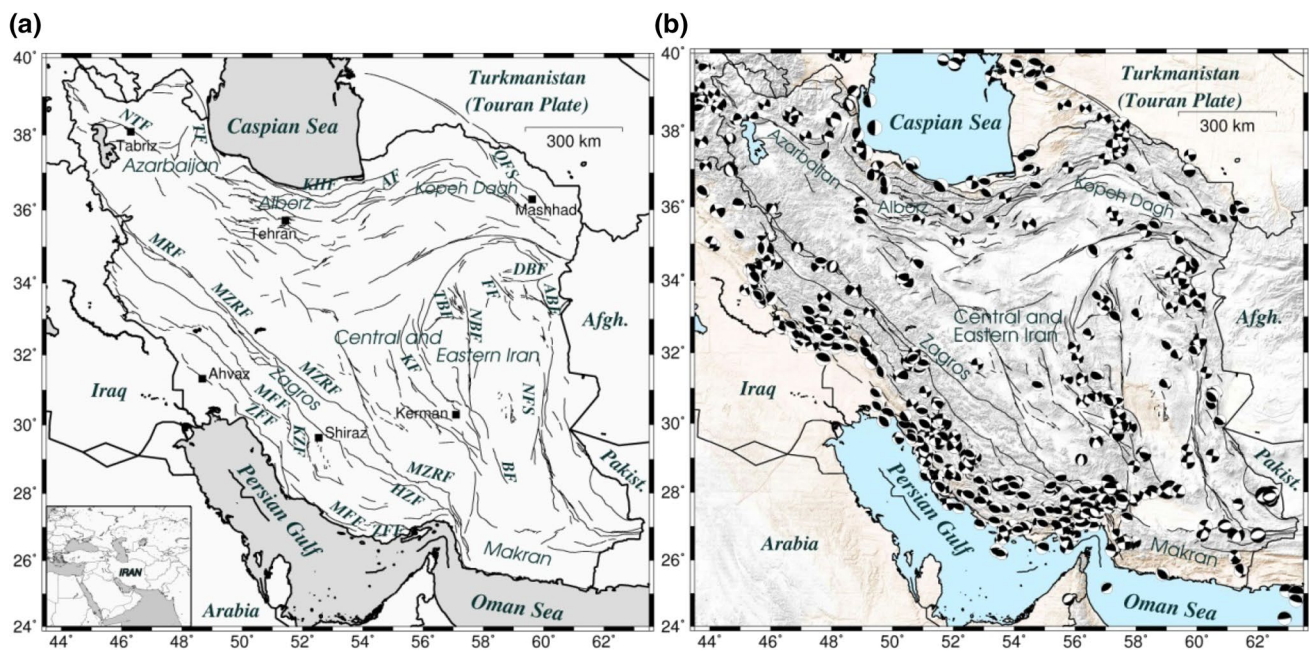


Fig. 1 **a** Active faults and major cities in seismotectonic provinces of Iran. *NTF* North Tabriz F., *TF* Talesh F., *KHF* Khazar (Caspian) F. and *AF*, *DBF*, *ABF*, *FF*, *TBF*, *KF*, *NBF*, *NFS*, *BF*, *MRF*, *MZRF*, *HZF*, *MFF*, *ZFF*, *KZF* and *TF*: are the Astaneh F., Dasht-e Bayaz F., Abiz F., Ferdows F., Tabas F., Kuhbanan F., Nayband F., Nehbandan

F. system, Bam F., Main Recent F., Main Zagros Reverse F., High Zagros F., Mountain Frontal F., Zagros Foredeep F., Kazeroun F. and Talesh F. The faults are adopted from the active fault map of Iran (Hessami et al. 2003a). **b** Focal mechanism of large Iranian earthquakes (GCMT, 2019)

recurrence interval of the earthquakes regarding a database with an adequate duration. An ideal seismic gap is essentially applicable for the earthquake prediction (Scholz 1990) as a supplementary material, since it is completely trapped between doughnut-shape of background seismicity in both sides along an active fault. According to the fact that separating the gaps is more or less influenced by personal judgments, some researchers questioned this method (e.g. Stuart and Aki 1988). Nonetheless, Ohtake et al. (1977, 1981) have investigated in a smart way the prediction of the 1978 earthquake in Oaxaca (Mexico) by using seismic quiescence. Empty spaces in space–time diagrams, which are near to the definition of a seismic gap, should be separated. This separation is completely relative. It depends on the density of seismicity in a space–time diagram.

Moreover, seismic migrations could be significantly distinguished along a fault strike using this method. The North Anatolian Fault in Turkey is a typical example of the migration of large earthquakes representing migration of six large earthquakes subsequently occurred between 1939 and 1967 from East to West (e.g. Scholz 1990). In Iran, the only active fault which has typically experienced migration of three historical earthquakes is the NTF (Berberian and Yeats 1999) (Fig. 1). As an example, in Iran, Gheitanchi and Raeissi (2004) investigated a short-term space–time diagram distinguishing lack of seismicity within the aftershock distribution of the 1997 Zirkuh-e Qaen earthquake (on the Abiz fault in East-Central Iran, EI) during three months.

Seismic cycle that may be recognized from space–time diagrams, was introduced by Fedetov (1965) and modified by Mogi (1977, 1985). It includes an aftershock sequence of the first earthquake, an intermediate-term seismic quiescence, the background seismicity, a short-term quiescence bounded with the mentioned background seismicity, an imminent foreshock sequence and finally the occurrence of the subsequent event (e.g. Scholz 1988; Ellsworth et al. 1981).

The space–time diagrams of earthquakes along the most active fault systems in Iran are investigated in this study. These faults are seismically active enough to show seismicity patterns. According to the continental behavior of the investigated earthquakes (IGUT catalog 2019) and the faults taken into account in this study, cut off magnitude which we will discuss and use for the earthquakes should be smaller than that of Lay et al. (1982).

The fault systems in this study are part of key structural elements in active tectonics of Iran (Fig. 2a, b). They have reasonably been chosen on the basis of their seismic activity, including background seismicity and large instrumental earthquakes that the fault systems have experienced in the past 8 years and in the current century, respectively. The faults are chronologically mature, thus they show their seismic behavior and stable seismicity pattern during geological periods. In this study, the location of the recent earthquakes

and also the moderate and large instrumental earthquakes are orthogonally projected to the fault plane in order to investigate whether a part of or the entire fault behaves seismically. It is important to notice that a seismic gap or a seismic cycle can rarely be found in their ideal forms in the world. In other words, ideal form of a gap means a gap completely surrounded by seismicity. The seismicity patterns taken into account in this paper are distinguished on the basis of the non-uniform and significant distribution of the earthquakes. The seismic gaps are displayed here by rectangles within the seismicity pattern. We have no reliable estimations of the size of imperfect and small seismic gaps, and the rectangle in the diagrams should be used only as a general guide. We have also investigated the remarkable migrations of the seismicity and the foreshocks and aftershocks lineaments related to the recent large earthquakes occurred in correspondence of the active faults.

Iranian active faults have not simultaneously been investigated using space–time diagrams, before. Seismicity patterns of this kind of diagrams are applicable as a precursor for prediction of earthquakes. According to the fact that prediction of earthquake is an important issue, the active faults, especially the faults associated with seismic cycles and specific seismicity patterns should be monitored. Monitoring of active faults includes definitely investigating space–time diagrams. The aim of this research is not directly prediction of earthquakes. It provides space–time diagrams as a complementary material and a general guide to distinguish specific seismicity patterns to help the process of prediction of earthquakes.

2 Tectonics, seismicity and faults

According to the most accepted classification, Persian plateau is divided into 5 major seismotectonics provinces; Alborz-Azarbaijan, Zagros, Kopeh-Dagh, East-Central Iran and Makran (Fig. 1). This classification is based on some parameters like seismicity, the earthquake focal mechanisms and GPS. Focal mechanisms in Alborz, Zagros and Kopeh-Dagh are reverse with sinistral component, reverse with dextral component and dextral, respectively. East-Central Iran also contains long right-lateral strike-slip faults. Maybe, with this definition, Azarbaijan area could be considered as a separate seismotectonic province. All of the Iranian seismotectonic provinces are host of some doublet and multiple earthquakes, which could be explained by the stress transferring phenomenon (e.g. Yazdanfar et al. 2018); for example: in E Iran the 31/08/1968 DB and 01/09/1968 Ferdows Eq.; the 1994 multiple Sefidabeh Eqs.; the 2010 Rigan doublet Eq.; the 2012 Ahar-Varzaghan doublet Eqs.; the 2017 triplet Hojedk Eqs. (e.g. Walker et al. 2013; Nemati 2017; Yazdanfar et al. 2018).

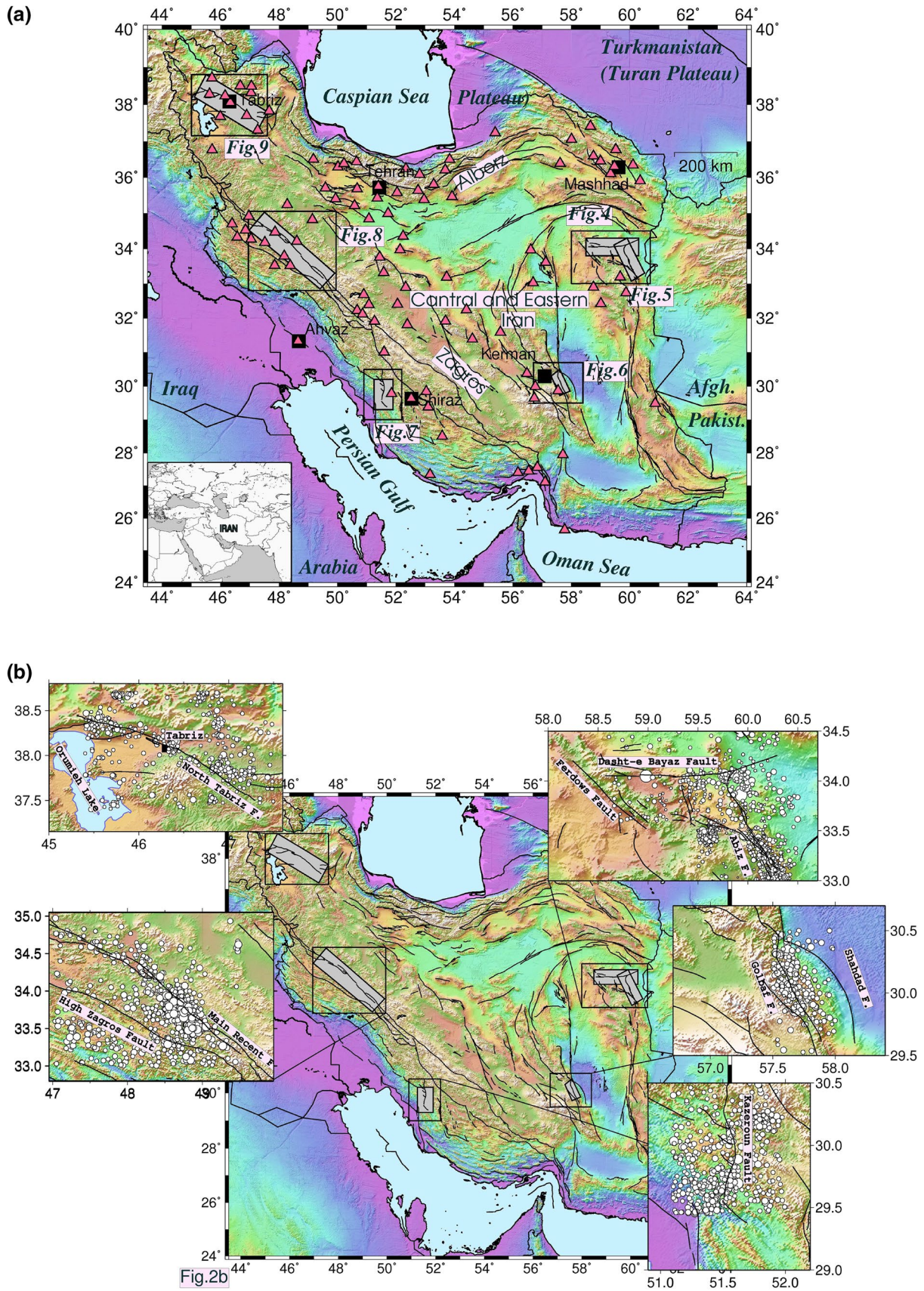


Fig. 2 a The active fault zones in three Persian seismotectonic provinces, Alborz-Azarbaijan, Zagros and EI and major cities in a greater detail. In this map the width of the gray rectangles (fault zones) is exaggerated. The triangles show the IGUT seismological stations. **b** Seismicity of the investigated fault zones

The next section focus on the three of the five seismotectonic provinces: Alborz-Azarbaijan, Zagros and East-Central Iran.

2.1 Alborz-Azarbaijan

One of the significant seismotectonic provinces of Iran, the Alborz Mountain range, which is South of the Caspian Sea, is roughly a high-elevated mountain belt (5671 m in summit). Folding and faulting in the Alborz has gradually been constructed since the Persian-Eurasia collision (Late Triassic; Jackson and McKenzie 1984). Many geological and seismological studies (e.g. Ritz et al. 2006; Nemati et al. 2011; Moradi et al. 2011; Nemati et al. 2013) have defined this broad seismotectonic province as a tectonically important active zone. The Central Alborz accommodates 5 mm/year shortening over 100 km, which is about 50% of the total shortening rate between central Iran and Eurasia (Vernant et al. 2004). The total amount of shortening in the center of the range has been estimated to be 30 km since the Pliocene (Allen et al. 2003). The east Alborz is under-thrusted southward by the South Caspian Basin, a remnant oceanic crust (e. g. Kadinsky-Cade et al. 1981), All faults in east Alborz, unlike the west part, are parallel to the range and participate in the shortening. The dominant mechanism of the earthquakes in Alborz is reverse with left-lateral component (e.g. Nemati et al. 2011).

The greatest instrumentally, the M_S 7.7 1990 Roudbar-Tarom event, in Iran have occurred in this province (Berberian et al. 1992). All faults in Alborz-Azarbaijan, including NTF, are parallel to the range and participate in its shortening (Allen et al. 2003). Moreover, Azarbaijan area is thought as a right-lateral tectonic system, which is located approximately between Anatolia and the Alborz range (Copley et al. 2013). Tectonic of Azarbaijan is characterized by a spatially distributed deformation with a shortening component. NNW Iran is characterized by N–S crustal shortening over about 500 km. Present-day geodynamic and geological framework resulted from a long geodynamic evolution started in the Early Triassic. Dominant mechanism of the earthquakes in Azarbaijan is right-lateral strike-slip (e.g. Moradi et al. 2011; Nemati 2013; Solaymani et al. 2019). Three consecutive and also destructive historical earthquakes (the 1721, 1780 and 1786 Eq. with the M_S 7.3, M_S 7.4 and M_S 6.3 Eq., respectively) occurred at NTF from the East to the West that makes it important amongst the other faults in Iran (Fig. 3a) (Berberian and Yeats 1999). Furthermore, from

paleoseismological studies Hessami et al. (2003b) found evidence for at least four events during the past 3.6 ka, as the most recent of which was the 1780 earthquake.

2.2 East-Central Iran (EI)

General features of the present-day tectonic and seismicity in EI have broadly been investigated. Major active strike-slip and thrust faults are remarkably observed in EI (e.g. Walker and Jackson 2004). They reported that total cumulative right-lateral shear displacement between Iran and Afghanistan resulted from these faults is about 75–100 km in length.

Tectonic of eastern Iran is dominated by large strike-slip faults, like Nayband, Kuhbanan and Lakar Kuh faults, which bounds the rigid aseismic blocks, i.e. Lut, Tabas, central Iran and Jazmourian (Fig. 1a). Lateral variations in the crust might be responsible for this kind of faulting. The detailed motion of rigid blocks is apparently controlled by their rigidity and forces on their sides. A significant characteristic of eastern Iran is that, majority of large earthquakes occurs on splay thrust faults separated from both ends of these strike-slip faults; e.g. the 2005 Zarand Eq. (Nemati and Gheitanchi 2011) and the 2017 Hojedk Eq. (Savidge et al. 2019).

Instrumental seismicity of EI is significantly concentrated over specific main patches. Within the important earthquake faults in EI, we could point to DB and Abiz faults that have experienced the 1968 DB (M_W 7.1) and the 1968 (M_W 6.3) Ferdows, the 1979 (M_W 7.1) Boniabad and the 1997 Zirkuh-e Qaen (M_W 7.1) mega-earthquakes. In the vicinity of this area the Tabas-e Golshan, M_S 7.7, catastrophic earthquake has struck EI in 1978 (Walker et al. 2011). Moreover, the most noticeably active areas in EI is Golbaf (Kerman province), which is a region with multiple conjunctions of fault zones. In this area the Nayband, Kuhbanan, Lakar Kuh and Shahdad faults as well as Golbaf fault, a super seismically active and also a multi-ruptured fault are present. Golbaf fault has typically experienced 5 intense earthquakes ($M_N > 5.7$) during 1981–2013 (Fig. 3b, c) (Berberian 2005; IGUT catalog). According to the paleoseismological investigations following digging a trench on the Golbaf fault, four paleo-earthquakes with magnitudes greater than 6.6 were identified (Basiri et al. 2013).

2.3 Zagros

Old hypothesis on Zagros tectonics (e.g. Berberian 1995) suggested that tectonic activity in the Zagros is concentrated on a few number of large, steeply dipping, and basement faults called “Master Blind Thrusts”. These faults can be extended into the lower sedimentary cover. This hypothesis is related to the fact that most large instrumental earthquakes in the Zagros can be related to one of these faults (Nissen et al. 2019). Hatzfeld et al. (2010) describes

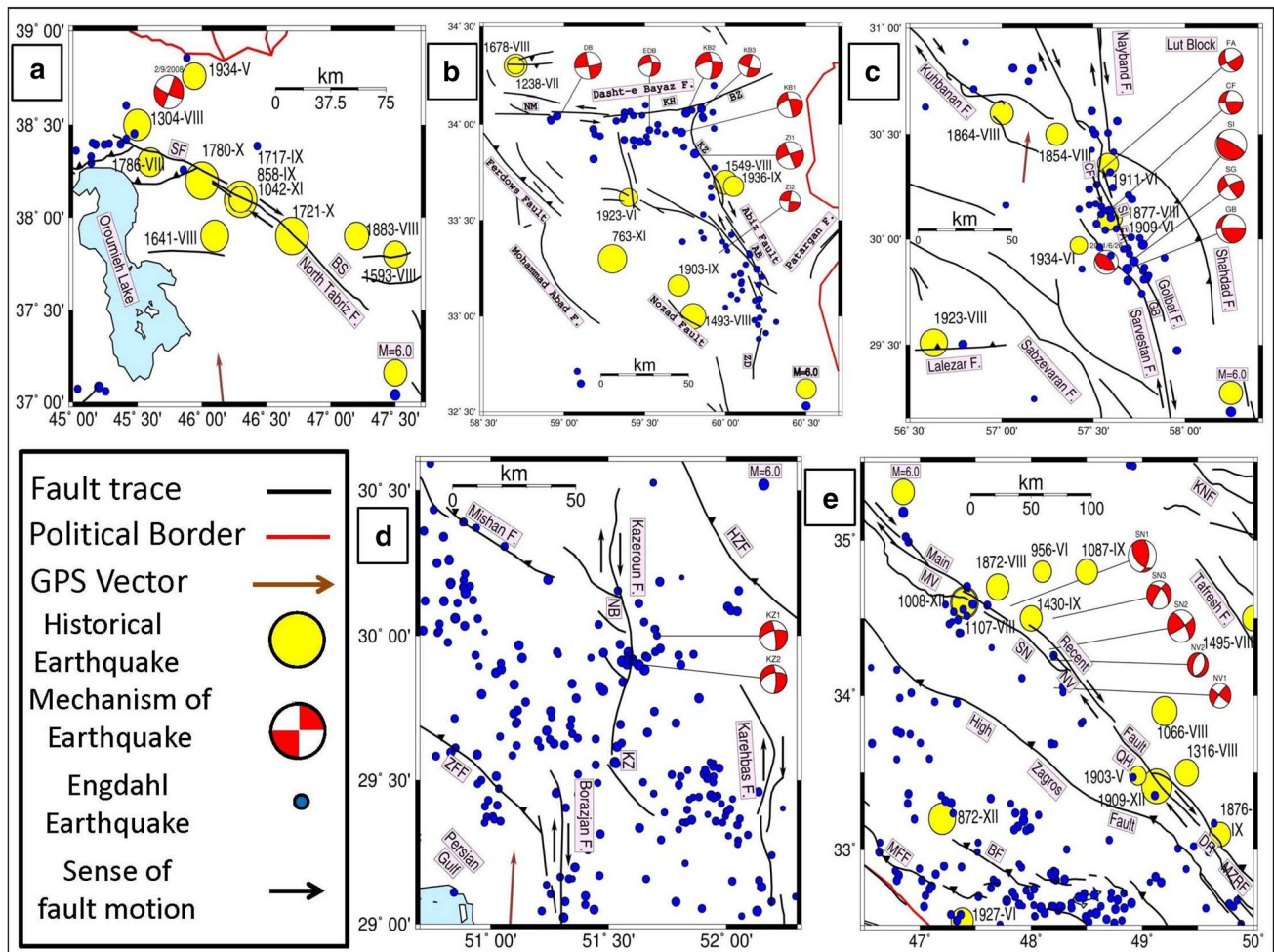


Fig. 3 Large scale seismotectonic maps for **a** Abiz-DB fault systems, **b** Golbaf fault, **c** Kazeroun fault, **d** Main Recent fault and **e** North Tabriz fault. Roman numbers indicate maximum intensity of the events (MMI scale). GPS velocity stations are 13.96, 20.99 and

11.96 mm/year for NTF, Kazeroun and Golbaf faults respectively (Vernant et al. 2004). Focal mechanisms are taken from GCMT, 2019. The abbreviations BF and KNF in **e** indicate the Balaroud Fault and Kushk-e Nosrat Fault, respectively

that seismicity and present-day deformation, based on tectonic, geomorphologic and geodetic data, concentrates near the 1000 m elevation contour, suggesting a relationship between basement and shallow deformations. This suggests a thick skinned tectonic deformation, which has southwestward propagated, starting from the MZRF (Fig. 1). Three long reverse and discrete faults (HZF, MFF and ZFF) with northeast dipping were moved to the south by steeply dipping right-laterally strike-slip faults (KZF) in the Zagros. The Zagros seismotectonic province has experienced many moderate reverse earthquakes (e.g. the M_w 5.9 Koodian Eq.; Nemati et al. 2012) without a mature surface rupture. The greatest instrumentally recorded earthquakes in Zagros was the 2017 Ezgeleh Kermanshahan M_w 7.4 Eq. (Nissen et al. 2019).

Zagros has many active faults experiencing strong seismicity, e.g. MRF and Kazeroun fault. Both faults move

strike-slip right-laterally. Several researchers (e.g. Berberian 1995, Talebian and Jackson 2004; Yamini-Fard et al. 2006) have introduced a relatively reasonable picture of seismotectonic and seismicity of Zagros. Seismic activity is roughly limited to the southern part of Zagros, and also to the MRF (NW of Zagros; Berberian 1995). Although, a major part of shortening due to convergence of Arabian-Persian plates is accommodated by Zagros thrust faulting (Berberian 1995), many devastating earthquakes have surprisingly occurred at the strike-slip faults; e.g. the 1909 Silakhour earthquake and 1957–1987 earthquakes on MRF and the two 1988 earthquakes on the Kazeroun fault (Fig. 1, 2, Tables 1, 2). Seismicity instantly stops beyond North of MRF in the Central Iran (Fig. 3d, e).

In all maps of Fig. 3 and Fig. 10, maximum intensity of the historical earthquakes (Roman numbers) were adopted from IIEES catalog, which were assembled from Ambraseys

Table 1 Catalogs used in this study

No	Catalog name	Duration	Specifications	Utilization
1	IGUT	After 2006	Including earthquakes	Seismicity pattern
2	IIEES	After 2004	Less earthquakes	Seismicity pattern
3	Engdahl	After 1961	Lack of earthquakes	Early large instrumental Eq
4	CMT of Harvard Un	After 1976	Lack of earthquakes	Focal mechanism

and Melville (1982), and Berberian and Yeats (1999) data in Modified Mercalli Intensity (MMI) scale.

It is important to note that although, epicentral area of the 1909 Silakhour event geologically is relied on Zagros, the properties of earthquakes in this area are completely different to the other side of the Zagros like the southern part.

3 Data and methods

The algorithm used in this study is a method of seismicity pattern applied for precursors of earthquakes (Scholz 1990). It is based on space–time diagrams which show seismicity patterns in resemblance to the ideal seismic cycle: a principal rupture is followed by an aftershock sequence. There is a post-seismic period of quiescence with duration of 50–70% of the total recurrence period of seismic cycle. This is followed by a general increase in background seismicity. Aftermath, this is sometimes followed by an intermediate-term quiescence, which typically extends over the entire the rupture. The rupture is usually surrounded by a doughnut pattern of seismicity. The rupture is preceded by immediate foreshocks a few weeks to days prior to the mainshock. The seismicity patterns also include migration of earthquakes.

In this part, an appropriate database is chosen within the Engdahl catalog, IGUT catalog, IIEES catalog, and local network data and relocated events with various methods. The Engdahl and IIEES catalogs are not as complete as that of the IGUT, considering the lack of small earthquakes in those databases. The local network data gathered from the active faults in Persia is just limited to the Qir-Karzin and Bam earthquake faults (Tatar et al. 2004), Kazeroun and Zendan-Minab faults (Yamini-Fard et al. 2006, 2007), Shahroud fault system (Nemati et al. 2011), NTF (Moradi et al. 2011) and Main Recent Fault (MRF) (Sepahvand et al. 2012) within a considerable number of active faults accommodating Arabia-Eurasia plate convergence in Iran (Fig. 1, 2). Because of this limitation (less number and short time duration of the networks) and also the fact that the short-term seismicity is only related to the aftershock data, we have to use and correlate all the only available data including small earthquakes (~ 8 years seismicity from the IGUT catalog), IIEES catalog, large instrumental earthquake (Engdahl et al. 1998, 2006) data, and Quaternary cumulative offsets along the active fault

systems (Table 1). The relocated events by using the *Mloc* (Multiple-Event Relocation Technique) are other candidate data having a reliable accuracy. Little is known about this method and also the published works in this case are so rare in Iran (e.g. Bergman and Solomon 1990; Walker et al. 2013). In addition, the greater magnitude of completeness for the Engdahl catalog makes the dataset incomplete, and therefore a considerable number of the earthquakes is not considered. Any space–time diagram must include the earthquakes. Only in this kind of diagram the seismicity pattern, including seismic quiescence, gap and seismic cycle could be found. Regarding rare data and also inadequate duration of local seismological networks in Iran, the IGUT catalog (a regional seismological network with adequate number of stations (139) in Iran, which releases earthquake data with a reliable accuracy) is the only available database, as a basic database, which could be convincingly investigated for the seismicity patterns related to the active faults. Moreover, the only suitable catalog for this purpose with data coming from numerous stations, considerable number of earthquakes, the greatest database in Iran with an appropriate magnitude of completeness, station coverage and acceptable location errors (< 5 km for dense areas (e.g. Nemati 2014) and < 10 km for areas with sparsely distributed stations, respectively; e.g. Walker et al. 2013) for the earthquakes, is IGUT. Regarding to the fault lengths (110–270 km for Golbaf and MRF, respectively), the location errors for the events used in this study in comparison to the fault lengths can be ignored and, therefore, could not definitely change the seismicity patterns to distinguish the gaps. Also, we add the earthquakes of IIEES catalog as a complementary material for our purposes. Naturally, a small part of the events having a little change in location could be duplicated, because two different seismological networks have located them (Table 1). Applying two different catalogs (one as base and the other as complementary material) for space–time diagrams are reasonable, when different locations for same earthquakes in diagrams do not change the seismicity pattern (gaps, migrations and...).

Gheitanchi and Raeissi (2004) found a short seismic gap (a few weeks) during three months of the aftershock sequence of the Zirkuh-e Qaen earthquake (M_w 7.2) occurred on 1997 May 10 on Abiz right-lateral strike-slip fault in EI. Furthermore, the well located earthquakes and

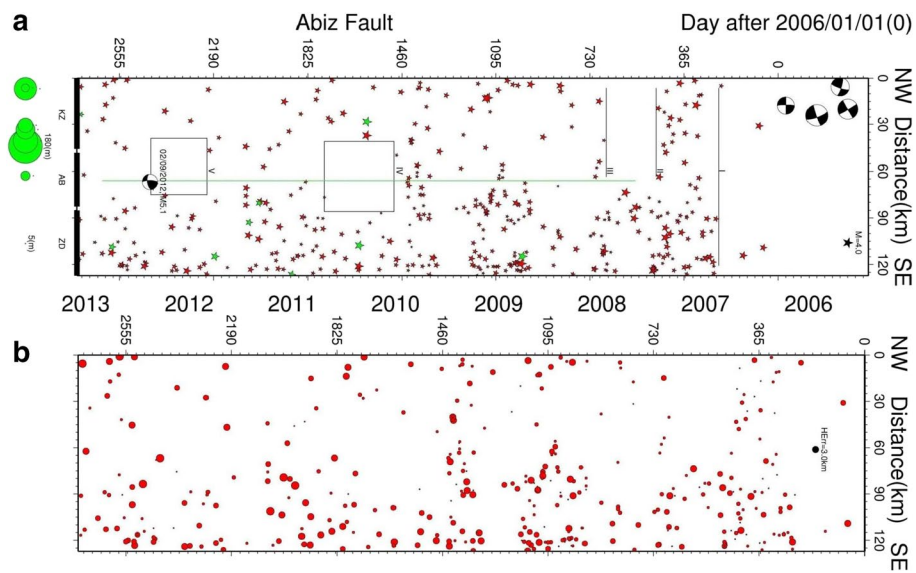
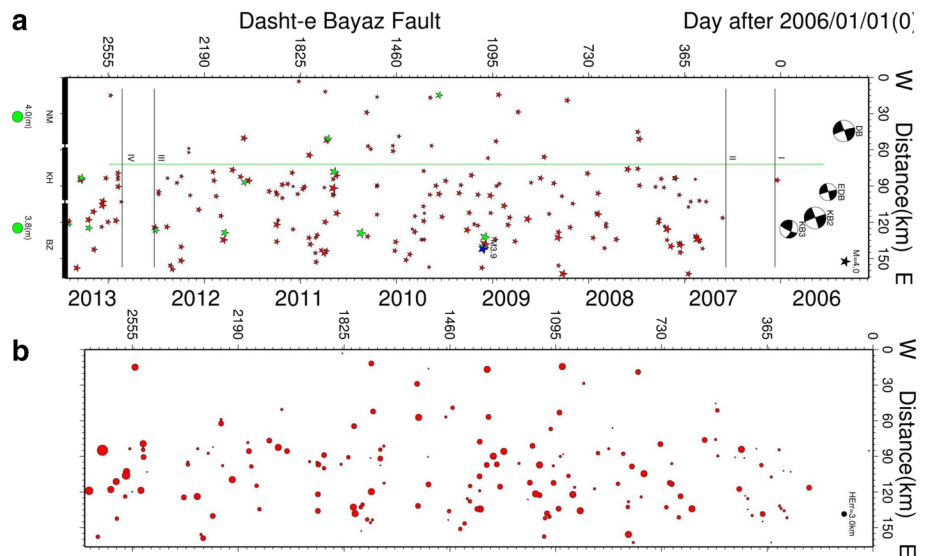


Fig. 4 **a** Seismicity of IGUT (red stars) along Abiz fault system with 125 km long in NE part of EI (Fig. 1). The blue and green stars after 2006 show the earthquakes with M_N magnitude greater than 4.0 and IIEES events (in Figs. 3a, 4a, 5a, 6a, 7a and 8a), respectively. Time axis is not scaled before 2006. Late Quaternary offsets (Berberian

et al. 1999) are shown by green circles (maximum and minimum values are in meter). The blue star in lower right part of the diagram is the magnitude legend for the earthquakes and the black thick lines show main geological segments. **b** Error diagram showing the data accuracy: RMS of the earthquakes

Fig. 5 **a** Seismicity along the DB fault system. The greatest earthquake is 2009/02/05 event with $M_N=3.9$. **b** Error diagram display RMS residuals related to the phases of the earthquakes



the reasonable accuracy of the locally recorded events, the durations of the aftershocks and also the background seismicity surveying (between eight weeks to six months in Iran) are not an adequate tool to evaluate intermediate- and long-term seismicity in comparison to the broad instrumental period.

In this paper, we used both significant instrumental earthquakes ($5.4 < M < 7.1$) that the fault systems have experienced between 1957 and 1998 (Engdahl et al. 1998) considering the history of strong activity of the fault and also

the seismicity after 2006. The earthquakes (with a distance less than 10 km from the fault plane) were orthogonally projected to the fault planes and were plotted versus time for each fault system. The historical earthquakes were not included in space–time diagrams because of the probable large errors in their location estimations (Fig. 3a–e) (Ambroseys and Melville 1982; Berberian and Yeats 1999).

Reliable results deduced by space–time diagrams (Figs. 4a, 5a, 6a, 7a, 8a and 9a) strongly depend on catalog completeness as well as location accuracy of the earthquakes

Fig. 6 **a** Seismicity along the Golbaf fault system in Southeast Iran. The geological segments are Chahar-Farsakh, CF; Sirch, SI; Fandogha, FA and Golbaf, GB. **b** RMS residuals of the earthquakes as diameter of the circles the errors range for

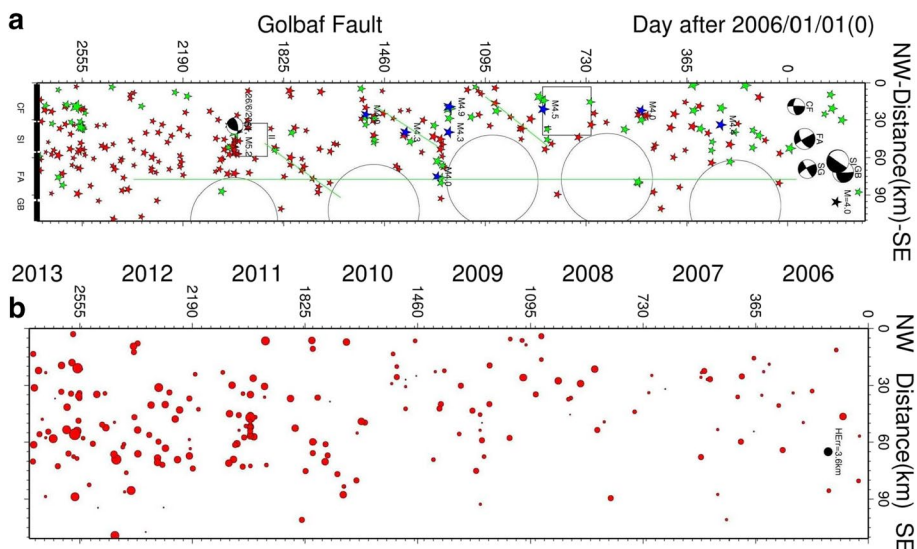
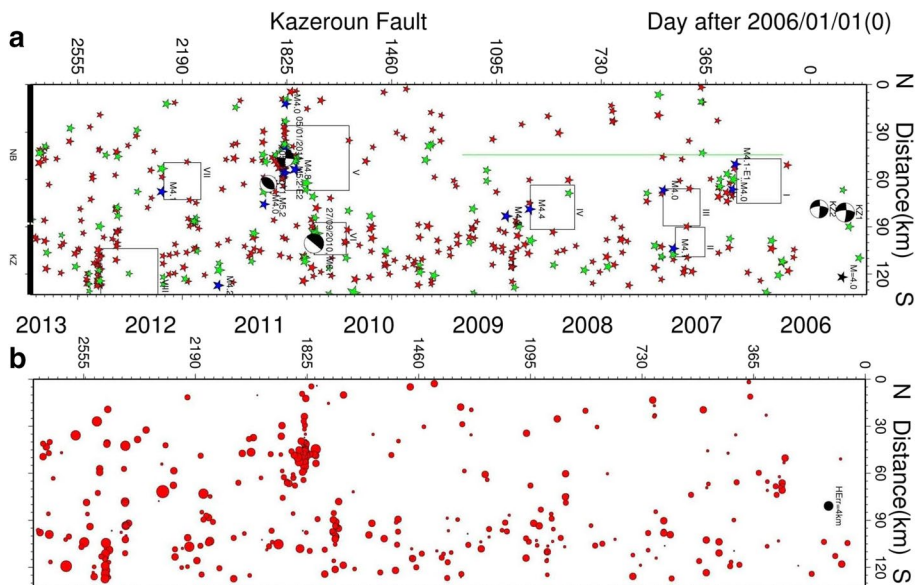


Fig. 7 **a** Seismicity along the Kazeroun fault system in the Zagros. The Kazeroun fault system has two geometrically separated segments (Noor-Abad, NB and Kazeroun, KZ) shown with the black thick lines. **b** Error diagram (RMS residual) display the error criteria of the earthquakes



in the database taken into account. For selecting the area seismic gaps in the space–time diagrams, we considered the bounded areas with earthquakes from all sides. Also only the remarkable empty areas in comparison to seismicity distribution and to the entire fault were considered.

For error estimation of the analysis, we evaluated the RMS residuals, number of P + S phases used for events locating and azimuthal gap of the earthquakes (the only error data released by the IGUT catalog) to display location error ranges of the earthquakes (Figs. 4b, 5b, 6b, 7b, 8b and 9b). The RMS residual of an event is not a perfect parameter for evaluating the location errors of the earthquakes. Average location errors of the events could be easily achieved by producing RMS into the average velocity of the P wave in the continental crust of the area (Havskov and Ottemöller 2010).

The average velocity of P wave is 7.1 km/s for NTF (Moradi et al. 2011), 6.1 km/s for Dasht-e Bayaz (DB) and Abiz (Walker et al. 2011), 5.9 km/s for Golbaf which is adapted from the nearest area, Bam (Tatar et al. 2005), 5.8 km/s for Kazeroun (Yamini-Fard et al. 2006) and 6.1 km/s for MRF (Sepahvand et al. 2012). This average velocity of P wave at each area is adapted from a dense local network. In the diagram of Figs. 4b, 5b, 6b, 7b, 8b and 9b the horizontal location error for each event in each area is plotted as the diameters of the red circles. The location errors for the earthquakes plotted in the diagrams are mainly less than 5.0 km.

The seismicity rates of the investigated faults are roughly different, they are related to different seismotectonic provinces (Berberian 1976), and also have different convergence rates as well as different tectonic and rheological properties

Fig. 8 **a** Seismicity along the MRF, the boundary between NW Zagros and central Iran. Morvarid (MV), Sahneh (SN), Nahavand (NV), Qal-e Hatam (QH) and Doroud (DR) are the geological segments of the fault (Tchalenko et al. 1974) which are characterized with the black thick lines in the diagram. **b** Error histograms of the events used for drawing space–time diagrams of MRF

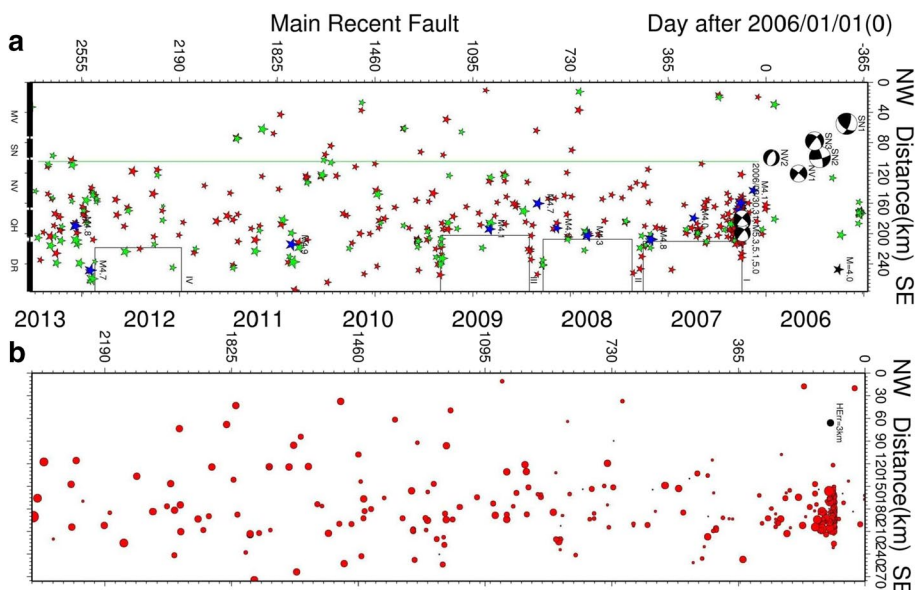
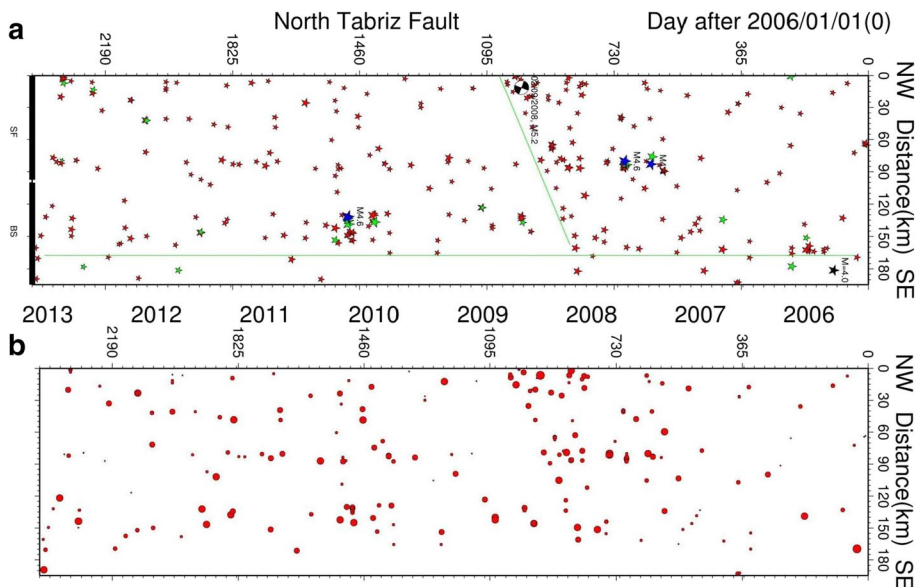


Fig. 9 **a** Seismicity along the NTF system. The blue stars show the earthquakes with M_N magnitude larger than 4.0. The Soufian (SF) and Basmenj (BS) segments are the main segments of the NTF system (Black thick lines). **b** RMS residual ranges of the earthquakes



of the crustal structure. Therefore, for comparing the seismicity of the faults with each other and presenting adequate number of the earthquakes in the seismicity pattern along the faults, variable cut-off magnitudes (M_C) for the earthquakes (>0.7 for the Abiz fault; DB fault >1.3 , Golbaf fault >1.7 ; Kazeroun fault, MRF and NTF >2.5 in M_N scale) were used, although the M_C is limited to IGUT released data in each area. IGUT catalog releases seismic data in each area according to the station distribution and its coverage. It means that number of earthquakes recorded with the network and their magnitude range are different from an area to another area.

It is important to note that only part of the events in Fig. 2 (closer than a distance of 10 km to the fault plane) was orthogonally projected to the fault surface. Each zone defined for the fault systems has a narrow width (20 km) centered with the main fault trace. According to the fact that the data were selected from Alborz-Azarbaijan, EI and Zagros seismotectonic provinces, seismotectonic setting of these areas are briefly explained. Figures 1 and 2 shows the active fault systems, seismological stations of IGUT, their relative zones in Iran map and also the earthquake epicenters used for the space–time and error diagrams, respectively.

Table 2 The large instrumental earthquakes occurred on the investigated active fault systems

No	Earthquake	Symb	Casulative F	Date	Lon. (°E)	Lat. (°N)	M _w	References
1	Sahneh1	SN1	MRF	13/12/1957	47.82	34.58	6.7	Talebian and Jackson 2002
2	Sahneh2	SN2	MRF	16/08/1958	48.17	34.3	6.6	Talebian and Jackson 2002
3	Sahneh3	SN3	MRF	24/03/1963	48.2	34.5	5.8	Talebian and Jackson 2002
4	Dasht-e Bayaz	DB	Dasht-e Bayaz	31/08/1968	58.98	34.05	7.1	Walker et al. 2004
5	E-Dasht-e Bayaz	EDB	Dasht-e Bayaz	11/09/1968	59.53	33.97	5.6	Walker et al. 2004
6	Kuli-Boniabad1	KB1	Abiz	14/11/1979	59.73	33.96	6.6	Walker et al. 2004
7	Kuli-Boniabad2	KB2	Dasht-e Bayaz	27/11/1979	59.76	34.06	7.1	Walker et al. 2004
8	Kuli-Boniabad3	KB3	Abiz-DB	7/12/1979	59.86	34.08	5.9	Walker et al. 2004
9	Golbaf	GB	Golbaf	11/06/1981	57.69	29.86	6.6	Berberian et al. 2001
10	Sirch	SI	Golbaf	28/07/1981	57.77	29.97	7.1	Berberian et al. 2001
11	Nahavand1	NV1	MRF	29/05/1987	48.21	34.05	4.9	Talebian et al. 2002
12	Kazeroun1	KZ1	Kazeroun	11/08/1988	51.71	30	5.9	Berberian 1995
13	Kazeroun2	KZ2	Kazeroun	6/12/1988	51.64	29.94	5.6	Berberian 1995
14	Sirch-Golbaf	SG	Golbaf	20/11/1989	57.71	29.9	5.9	Berberian et al. 2001
15	Zirkuh-e Ghaen1	ZI1	Abiz	10/05/1997	59.81	33.84	7.1	Berberian et al. 1999
16	Zirkuh-e Ghaen2	ZI2	Abiz	20/06/1997	59.96	33.33	5.4	Berberian et al. 1999
17	Fandogha	FA	Golbaf	14/03/1998	57.59	30.14	6.6	Berberian et al. 2001
18	Nahavand2	NV2	MRF	21/08/1998	48.16	34.23	4.9	Talebian and Jackson 2002
19	Chahar-Farsakh	CF	Golbaf	18/11/1998	57.53	30.32	5.4	Berberian et al. 2001

Location of the earthquakes are adopted from Engdahl et al. (1998)

Table 3 The intensity scale by Ambraseys and Melville (1982) and their equivalence in MMI scale

Amb. Scale	MM intensity
i1	X–XII
i2	VIII–IX
i3	VI–VII
i4	IV–V
i5	IV

4 Results: seismicity pattern

In this study, spatial and temporal seismicity view along the Abiz fault (660 earthquakes), Dasht-e Bayaz fault (285 earthquakes), Golbaf fault (220 earthquakes), Kazeroun fault (480 earthquakes), Main Recent Fault (705 earthquakes) and North Tabriz fault (505 earthquakes) have been investigated (Fig. 2 and Table 2). The mentioned faults are located in the three seismotectonic provinces of Iran. Each fault system was investigated separately and all of them are dipping near vertically. For this study, we assumed a specific zone for the faults with a specific width, in which the earthquakes could be convincingly related to the fault. The widths of the fault zones were defined as narrow as 20 km.

4.1 Abiz fault

Abiz right-lateral strike-slip fault system is remarkably home of the longest co-seismic rupture (the 1997 Zirkuh-e Qaen earthquake, M_w 7.1) documented in the Persian earthquakes (125 km; Berberian et al. 1999; Walker et al. 2011). Abiz and DB fault systems belongs to a noticeable seismically active area in EI (Fig. 4a) (e.g. Walker et al. 2011). The Northern part (separated with a green line in Fig. 3a) of Abiz fault (Korizan, KZ and Abiz, AB, segments specified with thick black lines; Fig. 4a) has experienced no intense seismicity during four years between 2006 and 2012/09 in comparison with the Southern segment (Zard-Alou, ZD, Fig. 4a). Surprisingly, the area with low rate of seismicity is associated with the epicentral areas of four significant earthquakes (ZI1, ZI2, KB1 and KB3; Table 2, Fig. 3d) including the 1997 Zirkuh-e Qaen (Berberian et al. 1999) earthquake. The entire Abiz fault system has experienced a relative seismic quiescence during 8 months since early 2006 (limited to the thin black line (I) in Fig. 4a). Three remarkable areas with few months lack of seismicity were also identified in 2007 (between line II and III), 2010 (rectangle IV) and 2012 (rectangle V). The middle part of the fault has experienced a seismic quiescence (in 2012) just before the

strong activation of 2012/09/02 (M_N 5.1) moderate earthquake without any considerable foreshock and aftershock. This result may not be related to the completeness level of the earthquakes (0.7 is small enough) or criteria of data selection. This quiescence has not been densely covered by the background seismicity. This fault system has also experienced a short-term seismic gap in 1997. A partial gap was found by Gheitanchi and Raeissi (2004) during three months of aftershock surveying for the 1997 Zirkuhe Qaen earthquake on the AB segment. Late Quaternary offsets (Green circles in Fig. 4a), which could be supposed as the long-term slip rate on the Abiz fault system (Berberian et al. 1999), has surprisingly a strong correlation with the less active segments of the fault. The maximum value of this cumulative offset (180 m) has occurred near three periods of seismic quiescence and also near the epicentral area of strong earthquakes. There is also a correlation between maximum quaternary slip and lower rate of interseismic seismicity on the KZ and AB segments. We must neglect smaller empty areas with seismicity gaps in comparison to the fault length in the diagrams. Figure 4a shows that the IIEES events (green stars) could not help us so much in this case (Table 3).

Average values of RMS, number of phases and also the gap azimuth of the database used for this fault shows a fairly monitoring and station coverage (Fig. 1). Figure 4b shows that the location accuracy achieved in this study is neglected in comparison with the fault length. The seismicity pattern is the same as that in Fig. 4a.

4.2 Dasht-e Bayaz fault

The DB fault system with a total length of 165 km and three segments (Nimbluk, NM; Khidbas, KH and Boznabad, BZ; Fig. 5a), lies in E–W direction and has a strike slip left-lateral kinematics with a near vertical dip (Ambraseys and Tchalenko 1969; Tchalenko et al. 1974; Walker et al. 2004, 2011). This fault system has experienced devastating earthquakes in the past century. The unique historical event in 1678 and also the 1968 DB instrumental event have occurred in the West of DB fault, and both the 1979 Boniabad (KB2 and KB3) and the 1968 East of DB (EDB) earthquakes (Table 2, Figs. 3b and 5a) have occurred in the Eastern part (Walker et al. 2004). Both strong and old instrumental seismicity and recent background seismicity ($M_N > 1.3$) demonstrate that the Eastern part (KH and BZ segments separated by a green line in Fig. 5a) of the DB fault system is remarkably more active than the Western segment (the NM). The Western part of the fault system has partially been activated between 2008 and 2011 within the overall seismic quiescence before 2008 and after 2011 (Fig. 5a). The entire fault has experienced two significant and remarkable seismic quiescence with 7 and 4 months duration, respectively, after

January 2006 (the area between black thin lines I and II) and July 2012 (the area between black thin lines III and IV). No migration of the seismicity was recorded along the fault during more than seven years of seismic surveying. Tchalenko et al. (1974) has measured the inter-seismic surface slip (Max. ~4 m) along the Western part of the fault, which is slightly greater than that of the Eastern part (green circles in Fig. 5a). There is a clear correlation between geologically separated segments and seismically active areas along DB fault. The NM segment may be slipping aseismically and maybe both the KH and BZ segments have been characterized with the seismic activity since 1968. Less number of the IIEES earthquakes does not complete IGUT seismicity pattern in Fig. 5a.

The data used for Fig. 5a are enough fairly accurate in illustrating the seismicity pattern along DB fault, as this area has a slightly better monitoring station coverage than the Abiz fault region (Fig. 2). The location accuracy diagram of Fig. 5b shows that patterns of seismicity have not been changed in comparison to Fig. 5a, which indicates the reliability of the data.

4.3 Golbaf fault

The Golbaf fault system is known as a multi-rupture and the most active continental fault (right-lateral strike-slip) in Persian Plateau in the past and present centuries (e.g. the 1981 Sirch earthquake, M_W 7.1) (e.g. Berberian 2005). For example, eight earthquakes with M_N magnitude greater than 4.0 have occurred along Golbaf fault during 4.5 years (blue stars after 2006 in Fig. 6a). The first aspect of Golbaf diagram illustrates the consecutive seismic gaps (open big circles), with a migration pattern of the seismicity. The seismicity has explicitly and also regularly migrated from the South–East to the North–West of the fault at least three times without any time overlapping during a three year period (2008/04–2011/04). These migrated patches of the seismicity (characterized by oblique green lines) show a gently southeastward shift. The southernmost segment (Golbaf, GB in Fig. 6a), separated by a long green line, is less active compared to the Northern segments (Chahar Farsakh, CF; Sirch, SI and Fandogha, FA in Fig. 6a). It seems that intense background seismicity and also a large earthquake and its foreshocks and aftershocks have occurred at the end of the last migration. An earthquake (2008, M_N 4.5) has occurred following ~6 months of seismic quiescence (rectangle I). Sirch earthquake (the 2011/06/26 Eq., M_N 5.2) has occurred following a few months of seismic quiescence (rectangle II) and at the end of a migration, after a few immediate foreshocks and also has been followed by numerous aftershocks ($M_N > 1.7$). Immediate foreshocks typically occur a few weeks to days prior to a main shock. The seismic quiescence (the rectangle II in 2011, Fig. 6a) has been completely

surrounded by the background seismicity. Main shock and aftershocks affected an area about 30 km from SI segment. Also, Fig. 6a shows the active segments of the fault are the host of the important large instrumental earthquakes occurred at Golbaf fault in the past century.

Berberian (2005) has pointed to the rupture patterns generated by large and moderate instrumental and historical earthquakes on Golbaf fault to evaluate the predictability of 2003 Bam catastrophic earthquake in the South–East of Iran. He started with the 1877 (5.6) earthquake, continued with the 1909 (5.5), 1911 (5.6), 1948 (6.0), 1969 (5.2), 1981/06/11 (6.7), 1981/07/26 (7.1), 1989 (5.7), 1998/03/14 (6.6) earthquakes and ended with the 1998/11/08 (5.4) event. Recurrence behavior and rare seismic traits of the seismicity on the Golbaf fault system are significant issues among the investigated faults in Iran.

Like DB fault area, Golbaf region is covered by the IGUT seismological stations (Fig. 2) of Kerman subnetwork. The accuracy of the data used for diagram of Fig. 6a indicate that majority of RMS, number of the phases, gap azimuths and depth of the events were placed in acceptable ranges. According to the error diagram of the Fig. 6b, the seismicity patterns, as well as seismic migrations, are still seen in Fig. 6a.

4.4 Kazeroun fault

The N-S Kazeroun fault system (~ 130 km long) consists of right-lateral strike-slip fault segments (Figs. 3b and 7a), which has cut and displaced the NW–SE directed thrust faults in the Zagros seismotectonic province (e.g. Berberian 1995). In the Zagros the seismicity is not exactly associated with the thrust faults; instead, it densely occurs on the strike-slip faults (e.g. Yamini-Fard et al. 2006). For example, six earthquakes with M_N magnitude greater than 4.0 have occurred along Kazeroun fault during 2.5 years (blue stars after 2006 in Fig. 7a and their gaps shown with rectangles I–IV). According to Fig. 7a the Southern segment of Kazeroun fault (Kazeroun, KZ, the black thick line) is more seismically active than the Northern segment (Noor-Abad, NB). Entire NB segment has experienced an absolute seismic silence from 2006/01 to 2006/09. On this fault system only two instrumental earthquakes (the 1988 KZ1 and KZ2 events, Fig. 7a and Table 2) have occurred in the modern history of seismicity. Following a lower rate of seismicity (3.5 years; the green line) on the NB segment, the Northern part of Kazeroun fault has experienced a 5.2 magnitude (M_N) event in 2011/01/05. This earthquake has occurred after almost seven months of quiescence (rectangle V). Almost 40 km manifest aftershock elongation with a few foreshocks is presented in Fig. 7a. Shortly after this earthquake another event (M_N 5.2) has occurred in the Southern vicinity of the previous one. The strongest earthquake related to Kazeroun

fault has occurred in 2010/09/27 with $M_N=6.1$ throughout this period on the KZ segment (with a gap of rectangle VI). Significantly, majority of the earthquakes with magnitude greater than 4.0 has occurred after a few months of seismic silence and have been mainly followed by a sequence of aftershocks (rectangles V–VIII in Fig. 7a). The 2010/09/27 aftershocks have elongated ~ 25 km. The background seismicity has roughly surrounded by few months of seismic quiescence before this earthquake. There is much number of the IIEES events (green stars), which are in correspondence with the seismicity patterns of IGUT.

When the seismic cycle occurred along the NB segment (the earthquakes of 2006/09/19 with $M_N=4.1$ as event 1 and also of 2011/01/05 as event 2 shown in Fig. 7a) is considered, a complete seismic cycle scenario similar to that of Scholz (1988) could not be seen. The seismic cycle scenario of Scholz (1988) represents a complete and ideal seismic gap, which is attributed to the training purposes and is difficult to be found in nature. This seismic cycle includes few months of seismic silence (before event 1, rectangle I), a short-term aftershock sequence (after event 1), a long diffused and sparse seismicity (from 2007/01 to 2010/05 between event 1 and 2), a short-term quiescence (6 months, rectangle V), an immediate foreshock sequence and finally the occurrence of event 2.

Figure 7b displays the seismicity patterns as well as Fig. 7a, because the location accuracy achieved in this manner ($RMS \times \tilde{V}_p$) is small enough to preserve the seismicity pattern.

4.5 Main recent fault

The ~ 270 km long MRF extends from 47° E, 35° N to 49.5° E, 33° N. This dextral strike-slip fault (Figs. 3e and 8a) is divided into several segments and separates the central Iran from northwestern Zagros (Tchalencko et al. 1974; Berberian 1995; Talebian and Jackson 2002). In 1909, MRF has experienced one of the largest historical earthquakes ever documented in Persia (the Silakhour earthquake, M_S 7.4) on Doroud segment (Ambraseys and Melville, 1982). Morvarid (MV), Sahneh (SN) and northern Nahavand (NV) segments in the North–West part of the fault (the first 110 km, separated with green line), which are the faults of the origin of the large instrumental earthquakes (the 1957 SN1, 1958 SN2, 1963 SN3, 1987 NV1 and the 1998 NV2 earthquakes), have been recently less active than the South–East parts (southern NV, Qal-e Hatam, QH and Doroud, DR segments, thick black lines in Fig. 8a). In the past 7.5 years, in the South–East parts of the MRF the most significant event was the 2006/03/31 earthquake (M_W 6.1) with a strong foreshock (the 2006/03/30 Eq., M_N 5.1) and a long (6 months) and intense aftershock sequences ($M_N > 2.5$). These sequences include seven events with M_N magnitude greater than 4.0 in

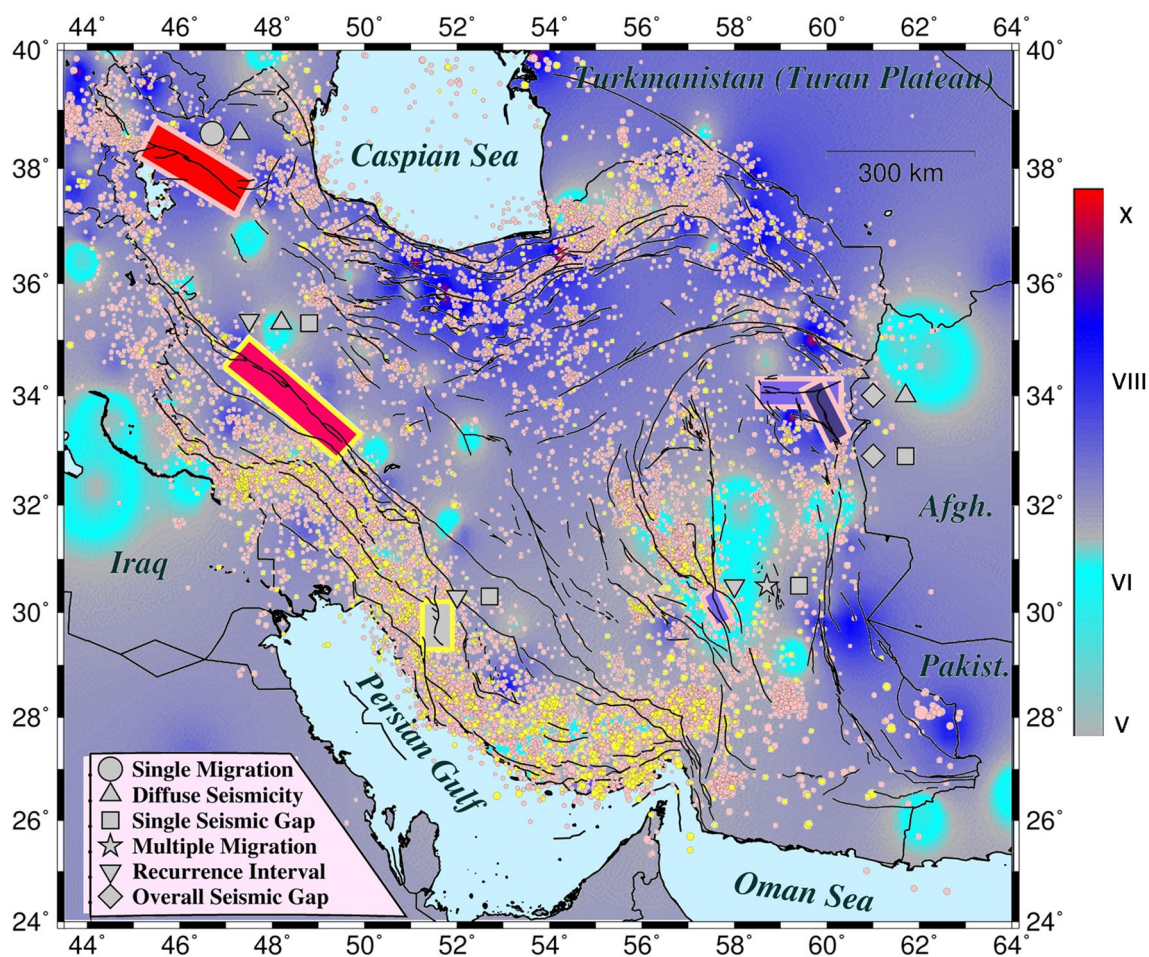


Fig. 10 Main results of this study. Small circles indicate IGUT earthquakes (2006–2016) with focal depth greater than 20 km (yellow) and less than 20 km (pink). Maximum depth of the earthquakes, shown by color of rectangle border (as the same as circles), are adapted

from local networks (see the text) and IGUT catalog. The background image map indicates intensity of the historical earthquakes. Color of rectangles shows maximum intensity in each area in accordance to the intensity bar of the map

the first month after the main shock (covered by the focal mechanisms in Fig. 8a). The aftershocks extension is about 70 km on the NV, QH and DR segments. This ruptured part of MRF remained active after the earthquake occurrence and has experienced 8 earthquakes with $M_N > 4.0$ during the next 7 years (Fig. 8a). The southeastern part of the fault has subsequently experienced 3 annual seismic gaps from 2006/03 to 2009/03 (three similar rectangles, I, II and III in Fig. 8a). After intense activation of this part of MRF, DR segment has experienced quiescence (1 year, rectangle IV) and has been shaken afterward by a M_N 4.7 earthquake in 2012/11/27 without felt foreshock and aftershock sequences. Sepahvand et al. (2012) obtained about 60 km for the elongation of the aftershocks for the 2006/03/31 earthquake. The MV and SN segments remained completely inactive from 2011/06, which could indicate the occurrence of a large earthquake at short term.

According to Fig. 8b error of seismicity parameters of the majority of the earthquakes used for plotting the space–time diagram of MRF are reliable. The location accuracy of this diagram shows the seismicity pattern and shapes for the empty areas are like those of Fig. 8a. Regarding these statistical diagrams, it seems that MRF data is statistically more reliable in comparison to that of the other faults.

4.6 North Tabriz fault

The historical earthquakes of the NTF system have attracted much attention from the researchers (e.g. Berberian and Yeats 1999). The ~200 km NTF has a high fault slip rate of ~7.3 mm/year (Rizza et al. 2013). It is a unique example for historical earthquakes; e.g. the 1042 (M_S 7.3), the 1304 (M_S 7.3), the 1721 (M_S 7.3), the 1780 (M_S 7.4) and the

1786 (M_S 7.4) Eqs. (Ambraseys and Melville 1982). The last three earthquakes have ruptured NTF subsequently from the South–East to the North–West (Berberian and Yeats 1999). This is the only large earthquake migration ever documented in Iran.

The recent seismicity is uniformly distributed along NTF (Fig. 9a). Surprisingly, this fault has experienced less strong seismicity during the modern instrumental period. No significant gap related to earthquakes could be extracted from the seismicity pattern of this fault. Remarkably, the migration of the seismicity ($M_N > 2.5$) from the South–East to North–West during 2008–2009 (displayed with oblique green line) is seen in this fault. The southeastern termination of the fault is not much active (Fig. 9a). There are not much IIEES events (green stars) in this diagram.

Average values for error of the earthquake locations for NTF diagrams are acceptable. According to the diagram of Fig. 9b, the seismicity migration is distinguishable as well

as in the diagram of Fig. 9a. Therefore, the accuracy of our calculations and investigations for this fault is in an acceptable and reasonable range.

Figure 10 summarizes the results of this study. NTF is characterized by a single seismic migration, while Golbaf fault has experienced multiple seismic migrations during ~8 years. Earthquakes on Golbaf fault, Kazeroun fault and MRF have occurred with recurrence intervals. It is worth noting that overall seismic gaps are dominated by the two neighboring faults (DB and Abiz) in East-Central Iran. The background image map in Fig. 10 shows that Northern Iran is characterized by higher intensities than the South, which is not due to much more historical earthquakes occurred in the North, rather than to the distributions of Iran population. Totally, existing recurrence intervals in Kazeroun and Golbaf faults and MRF and the overall seismic gap in the DB and Abiz faults in East-Central Iran may indicate that Southern Iran shows a

Table 4 Seismic characteristics along the active faults taken into account in this study

Row	Name	Earthquake/Gap			Gap (Day)		Explanation
		Date	M	Mechanism	Depth	Rupture (km)	
1	Abiz	2007	–	–	–	293	A clear gap without a large earthquake
2		23/9/2008	4.2	–	13	–	An earthquake without a clear gap
3	DB	2010	–	–	–	212	A clear gap without a large earthquake
4		2/9/2012	5.1	Strike-Slip	–	217	A large Eq. with a clear gap and without a lineament of aftershocks
5		2006	–	–	–	119	A clear and thoroughly gap without a large earthquake
6		2012	–	–	–	186	A clear and thoroughly gap without a large earthquake
7	Golbaf	2006	–	–	–	335	A clear gap without a large earthquake
8		2007–2008	–	–	–	328	A clear gap without a large earthquake
9		4/6/2008	4.5	–	–	173	An earthquake with a clear gap
10		2008–2009	4.0	–	–	358	An earthquake with a clear gap
11		2009–2010	–	–	–	366	A clear gap without a large earthquake
12		2011	–	–	–	380	A clear gap without a large earthquake
13	Kazeroun	26/06/2011	5.2	Reverse	27	119	A large Eq. with a doughnut-shape gap and a lineament of aftershocks
14		19/09/2006	4.1	–	28	154	An earthquake with a clear gap
15		23/04/2007	4.1	–	–	151	An earthquake with a clear gap
16		28/05/2008	4.0	–	–	179	An earthquake with a clear gap
17		5/9/2008	4.4	–	–	158	An earthquake with a clear gap
18		27/09/2010	6.1	Reverse	20	115	A large Eq. with a doughnut-shape gap and a lineament of aftershocks
19		5/1/2011	5.2	Strike-Slip	39	225	A large Eq. with a doughnut-shape gap and a lineament of aftershocks
20		11/3/2012	4.1	–	–	130	An earthquake with a clear gap
21	MRF	18/10/2012	3.4	–	25	202	A lineament of seismicity with a partially seismic silence
22		6/3/2007	4.8	–	–	367	An earthquake with a partially seismic silence
23		2007–2008	–	–	–	335	A clear gap without a large earthquake
24		2008–2009	–	–	–	335	A clear gap without a large earthquake
25	NTF	27/11/2012	4.7	–	–	386	An earthquake with a clear gap
26		1/12/2007	4.6	–	10	60	An Eq. with a lineament of aftershocks and without a specific gap
27		2/9/2008	5.2	–	–	–	A large earthquake at the end of a seismicity migration
28		2/2/2010	4.6	–	7	62	An Eq. with a lineament of aftershocks and without a specific gap

more regular pattern of seismicity than the North, except for the migration of seismicity.

5 Discussion and conclusions

A time span of 8 years appears to be a very short time interval to investigate the seismic cycle of a large event on an active fault using space–time diagrams. It is impossible to obtain reliable results on the complete seismic cycle and long-term forecasting data, including the maximum magnitudes that the fault systems can host. Short-term forecasting, considering moderate events in active seismic areas, could be assessed in this research.

It is remarkable that earthquakes of M_N 5.2 have occurred in 2008/09/02 and 2011/06/26, at the end of a seismic migration near Northern part of NTF and Golbaf F., respectively. This may be due to a northwestward seismic stress migration associated with seismic stress growth along NTF and Golbaf F., which has been discharged with an occurrence of a large earthquake.

Kanamori and Anderson (1975), Mogi (1985), Wyss and Habermann (1988) and Scholz (1988) obtained direct relationships between duration of a seismic quiescence and magnitude of the related earthquake. Remarkable scatter in their data makes these relationships unsatisfactory. The durations for the seismic silences before some large earthquakes in Iran are 115 days for the 2010/09/27 event (M_N 6.1, Kazeroun F.), 225 days for the 2011/01/05 event (M_N 5.2, Kazeroun F.), 119 days for the 2011/06/26 event (M_N 5.2, Golbaf F.) and 217 days for the 2012/09/02 event (M_N 5.1, Abiz F.).

There are reliable linear relationships between the logarithm of the sub-surface rupture length and the magnitude of an earthquake, globally (Wells and Coppersmith 1994) and for Iran earthquakes (Nemati and Tatar 2015), respectively. If the aftershocks elongation for an earthquake is supposed as the rupture length at the depth (depth rupture), the depth rupture for the largest earthquakes occurred in 2010/09/27 (M_N 6.1, Kazeroun F.), 2011/01/05 (M_N 5.2, Kazeroun F.) and 2011/06/26 (M_N 5.2, Golbaf F.) was 20, 39 and 27 km, respectively (Table 4), which are slightly greater than the surface rupture and do not exactly follow the aforementioned relationships.

Short-term seismicity is an important issue because of its supplemental application in seismic hazard assessments and tectonics prediction of the earthquakes. Tectonically prediction estimates the earthquake occurrence by using seismic and geological behaviors of the fault systems. For the investigation of longer-term seismicity on active faults, a longer duration database should be used and a smaller cut-off magnitude could therefore be taken into account for each fault. Seismic quiescence and seismicity migration, which occur along an active fault, could be used as a complementary

material for seismic hazard assessment, as well as earthquake short-term predictions.

This study confirms the fact highlighted in other researches that the active faults in different seismotectonic provinces in Iran behave in different seismic manners. NTF and DB fault are less active than the others. In Abiz fault and MRF, the instrumental large earthquakes (e.g. the 1957 and 1958 Nahavand and 1997 Zirkuh earthquakes) have occurred on the recently less active parts of the faults, while in the Golbaf and DB fault systems the large seismicity (e.g. the 1968 DB and 1981 Sirch earthquakes) has occurred on the recently active segments of the faults. Comparing the faults also highlights the fact that Golbaf fault is significantly characterized by smaller spatial and temporal seismic quiescence. The Kazeroun fault system has experienced five large instrumental earthquakes (both the 1988 M_N 5.6–5.9, the 2010 M_N 5.0 and the 2011 M_N 5.2 earthquakes). Seismicity pattern for MRF reveals that more than 70% of the seismic energy has been released on less than 30% of the fault length from 2006 during a period of 8 years.

A possible explanation of the correlation between maximum quaternary slip and epicentral areas of early strong earthquakes on the KZ segment of Abiz fault, is that this segment could be aseismic, at least, during the recent period.

The most significant feature of the Persian large earthquakes ($M > 5.0$) occurred in correspondence of the investigated faults during 8 years suggests that mostly have occurred after a few months of seismic silences, and also have mainly associated with a few foreshocks. Moreover, most of the mentioned earthquakes have been followed by intense sequences of aftershocks. There is usually asymmetry before and after the large earthquakes in space–time diagrams. It helps to distinguish the sequences easier. The second result could be related to a specific rheology of the seismogenic part of the crustal structure.

Significantly, both migration patterns along Golbaf fault and NTF were interrupted by a large earthquake ($M > 5.0$). This is due to a seismic stress migration with a probable directive growth. NTF has only experienced one large earthquake in the instrumentally period and shows diffuse seismicity in most of the investigated time period. Because of better station distribution, data of Kazeroun fault, MRF and also NTF have more normal distributions for the gap azimuth histograms in comparison with the Abiz, DB and Golbaf fault systems. Duration of seismic gap of the earthquakes with $M_N > 4.5$ on NTF is less than 3 months and 2008 event of M_N 5.2 has occurred without a specific gap. According to the long seismic stress discharge of the aftershock sequence of the 2006 M_N 6.1 event in the southern part of the fault and the location of large earthquakes (1957–1998) in the northern part, it can be concluded that the seismic activity migrated southeastward, accordingly on the MRF.

Other significant issue is that all NTF, MRF and DB fault in Northern Iran had diffuse seismicity in their pasts, while Abiz, Kazeroun and Golbaf faults in the South had a single seismic gap. Both Abiz and Dasht-e Bayaz neighboring faults in East-Central Iran have experienced overall seismic gaps during the studied period. East to West migration of the earthquakes on NTF is in accordance to an East to West large seismicity migration in Northern Iran (Koppeh Dagh-Alborz-Azarbaijan), as described in Nemati (2015).

A clear relationship could not be found between seismic gap duration and the size of related earthquakes in Iran. Also, considering the aftershock elongation as depth rupture for a large earthquake, a reliable relationship could not be seen between depth rupture and size of an earthquake in Iran. This is due to the fact that adequate earthquake data in both cases does not exist.

Therefore, monitoring seismic migrations along an active fault, seismic silences and also imminent events afterward gives us a significant insight for seismic hazard and prediction of the earthquakes. Long monitoring of the active faults with local seismological networks could effectively address us to seismic hazard investigations and at least decrease the damages due to the strongly activation of the active faults.

Acknowledgements Thanks the IGUT and IIEES for their online recent earthquake catalogs (2006 to 2013). All the diagrams, histograms and maps were generated using the GMT software (Wessel and Smith 1998).

References

- Allen, M. B., Ghassemi, M. R., Shahrabi, M., & Qorashi, M. (2003). Accommodation of late Cenozoic oblique shortening in the Alborz range, Iran. *Journal of Structural Geology*, 25, 659–672.
- Ambraseys, N., & Melville, C. (1982). *A History of Persian Earthquakes* (p. 107). Cambridge: Cambridge University Press.
- Ambraseys, N., & Tchalenko, J. S. (1969). The Dasht-e-Bayas (Iran) earthquake of August 31, 1968: A field report. *Bulletin of the Seismological Society of America*, 59, 1751–1792.
- Basiri, M., Nazari, H., Foroutan, M., Solaymani, A. S., Shokri, M. A., Talebian, M., et al. (2013). Determination of clustering pattern of paleoearthquakes occurrences on the Golbaf Fault, SE Kerman. *Scientific Quarterly Journal of Geosciences*, 22(87), 171–180.
- Berberian M. (1976). Contribution to the seismotectonics of Iran. Part II. *Geological Survey of Iran (GSI)*, Report No. 39.
- Berberian, M. (1995). Master blind thrust faults hidden under the Zagros folds: Active basement tectonics and surface morphotectonic. *Tectonophysics*, 241, 193–224.
- Berberian, M. (2005). The 2003 Bam urban earthquake: A predictable seismotectonic pattern along the western margin of the rigid Lut block, southeast Iran. *Earthquake Spectra*, 21(1), 35–99.
- Berberian, M., Jackson, J. A., Qorashi, M., Khatib, M. M., Priestley, K., Talebian, M., et al. (1999). The 1997 May 10 Zirkuh (Qa' enat) earthquake (M 7.2): Faulting along the Sistan suture zone of East-Central Iran. *Geophysical Journal International*, 136, 671–694.
- Berberian, M., Qorashi, M., Jackson, J. A., Fielding, E., Parsons, B. E., Priestley, K., et al. (2001). The 1998 March 14 Fandoqa earthquake M=6.6 in Kerman, southeast Iran: Re-rupture of the 1981 Sirch earthquake fault, triggering of slip on adjacent thrusts, and the active tectonics of the Gowk fault zone. *Geophysical Journal International*, 146(2), 371–398.
- Berberian, M., Qorashi, M., Jackson, J., Priestley, K., & Wallace, T. (1992). The Roudbar-Tarom earthquake of 20 June 1990 in NW Persia: Preliminary field and seismological observations, and its Tectonic significance. *Bulletin of the Seismological Society of America*, 82(4), 1726–1755.
- Berberian, M., & Yeats, R. S. (1999). Patterns of historical earthquake ruptures in the Iranian Plateau. *Bulletin of the Seismological Society of America*, 89, 120–139.
- Bergman, E. A., & Solomon, S. C. (1990). Earthquake swarms on the Mid-Atlantic Ridge: Products of magmatism or extensional tectonics? *Journal of Geophysical Research*, 95, 4943–4965.
- Campos, J., Hatzfeld, D., Madariaga, R., Lopez, G., Kausel, E., Zollo, A., et al. (2002). A seismological study of the 1835 seismic gap in south-central Chile. *Physics of the Earth and Planetary Interiors*, 132, 177–195.
- Copley, A., Faridi, M., Jackson, J., Nazari, H., Ghorashi, M., Oveisi, B., et al. (2013). The 2012, August 11 Ahaz earthquakes: Consequences for tectonics and earthquake hazard in the Turkish-Iranian Plateau. *Geophysical Journal International*, 196, 15–21.
- Ellsworth, W. L., Lindh, A. G., Prescott, W. H., & Herd, D. G. (1981). The 1906 San Francisco earthquake and the seismic cycle. In *Earthquake prediction. An international review* (pp. 223–246). Washington D.C.: American Geophysical Union.
- Engdahl, E. R., Jackson, J. A., Myers, S. C., Bergman, E. A., & Priestley, K. (2006). Relocation and assessment of seismicity in the Iran region. *Geophysical Journal International*, 167, 761–778.
- Engdahl, E. R., Vander Hilst, R. D., & Buland, R. P. (1998). Global teleseismic earthquake relocation with improved travel time sand procedures for depth determination. *Bulletin of the Seismological Society of America*, 88, 722–743.
- Fedotov, S. A. (1965). Regularities of the distribution of strong earthquakes in Kamchatka, the Kuril Islands, and the north-east Japan. In *Seismic Microregionalization*. Transactions of the Institute of Physics of the Earth, Academy of Sciences of the USSR (Trudy Instituta Fiziki Zemli, Akademiya Nauk SSSR), No. 36, pp. 66–93 [in Russian].
- Gheitanchi, M. R., & Raeesi, M. (2004). Analysis of the 1997 Zirkuh (Ghean-Birjand) aftershock sequence in east Iran. *Acta Seismologica Sinica*, 17(1), 38–46.
- Hatzfeld, D., Authemayou, C., van der Beek, P., Bellier, O., Lavé, J., Oveisi, B., et al. (2010). *The kinematics of the Zagros Mountains (Iran)* (Vol. 330, pp. 19–42). London: Geological Society.
- Havskov, J., & Ottemöller, L. (2010). *Routine data processing in earthquake seismology, with sample data, exercises and software*. Dordrecht, Heidelberg, London, New York: Springer.
- Hessami K., Jamali F., and Tabassi H. (2003a). Map of Major Active Faults of Iran. Tech. rep., International Institute of Earthquake Engineering and Seismology (IIEES), internal report, <https://www.iiees.ir>.
- Hessami, K., Pantosti, D., Tabassi, H., Shabaniyan, E., Abbassi, M. R., Feghhi, K., et al. (2003b). Paleoeearthquakes and slip rates of the North Tabriz Fault NW Iran: Preliminary results. *Annals of Geophysics*, 46, 903–915.
- IGUT catalog. (2019). Institute of Geophysics University of Tehran, IGUT. <http://irsc.ut.ac.ir>
- Jackson, J., & McKenzie, D. (1984). Active tectonics of the Alpine-Himalayan Belt between western Turkey and Pakistan. *Geophysical Journal of the Royal Astronomical Society*, 77, 185–264.
- Kadinsky-Cade, K., Barazangi, M., Oliver, J., & Isacks, B. (1981). Lateral variations of high-frequency Seismic wave propagations at regional distances across the Turkish and Iranian plateaus. *Journal of Geophysical Research*, 86, 9377–9396.

- Kanamori, H., & Anderson, D. C. (1975). Theoretical basis of some empirical relations in seismology. *The Bulletin of the Seismological Society of America*, 65, 1073–1096.
- Lay, T., Kanamori, H., & Ruff, L. (1982). The asperity model and nature of large subduction zone earthquakes. *Earthquake Prediction Research (Japan)*, 1, 3–71.
- Mogi, K. (1962). Magnitude–frequency relationship for elastic shocks accompanying fractures of various materials and some related problems in earthquakes. Bulletin of the Earthquake Research Institute, University of Tokyo, Vol. 40, pp. 831–883.
- Mogi, K. (1977). Seismic activity and earthquake prediction. In *Earthquake prediction symposium, Tokyo*, 203–14.
- Mogi, K. (1985). *Earthquake prediction*. Tokyo: Academic press.
- Moradi, A., Hatzfeld, D., & Tatar, M. (2011). seismicity and seismotectonics of the North Tabriz fault (Iran). *Tectonophysics*, 506, 22–30.
- Nemati, M. (2013). Some aspects about seismology of 2012 August 11 Ahar-Vaezaghan (Azarbayjan, NW Persia) earthquakes sequences. *Journal of Sciences, Islamic Republic of Iran*, 24(3), 229–241.
- Nemati, M. (2014). An appraisal of aftershocks behavior for large earthquakes in Persia. *Journal of Asian Earth Science*, 79(A), 432–440.
- Nemati, M. (2015). Intermediate-term variations in 200 years seismicity in north of Iran. *The Journal of Seismology*, 19, 585–605.
- Nemati, M. (2017). Sequence signal processing of 2012 Ahar-Vaezaghan earthquake (MW 6.4) of NW Iran. *Environmental Earth Sciences*, 76(495), 1–12.
- Nemati, M., & Gheitanchi, M. (2011). Analysis of 2005 Dahuieh (Zarand) aftershocks sequence in Kerman province. *Journal of Earth and Space Physics, Institute of Geophysics of University of Tehran*, 37(1), 1–9.
- Nemati, M., Hatzfeld, D., Gheitanchi, M., Sadidkhouy, A., & Mirzaei, N. (2011). Microseismicity and seismotectonics of the Firouzkuh and Astaneh faults (east Alborz, Iran). *Tectonophysics*, 506, 11–21.
- Nemati, M., Hollingsworth, J., Zhong, W., Bolourchi, M. J., & Talebian, M. (2013). Microseismicity and seismotectonics of the South Caspian Lowlands, northeast of Iran. *Geophysical Journal International*, 193, 1053–1070.
- Nemati, M., Oveisi, B., Foroutan, M., & Bolourchi, M. J. (2012). Geomorphology and seismology of MW=5.8 Koodian earthquake, Southeast Zagros. *Quarterly Journal of Geoscience, Geological Survey of Iran*, 85, 81–88.
- Nemati, M., & Tatar, M. (2015). Relations between source parameters for large Persian earthquakes. *Annals of Geophysics*, 58(5), S0543. <https://doi.org/10.4401/ag-6665>.
- Nissen, E., Ghods, A., Karasözen, E., Elliott, J. R., Barnhart, W. D., Bergman, E. A., et al. (2019). The 12 November 2017 Mw 7.3 Ezgeleh-Sarpolzahab (Iran), Earthquake and active tectonics of the Lurestan arc. *Journal of Geophysical Research Solid Earth*, 124, 1–19.
- Ohtake, M., Matomoto, T., & Latham, G. (1977). Seismicity gap near Oaxaca, southern Mexico as a probable precursor to a large earthquake. *Pure and Applied Geophysics*, 115, 375–385.
- Ohtake, M., Matomoto, T., & Latham, G. (1981). *Evaluation of the forcast of the 1978 Oaxaca, southern Mexico earthquake based on a precursory seismic quiescence. An international review* (pp. 53–62). Washington D.C.: American Geophysical Union.
- Ritz, J. F., Nazari, H., Ghassemi, A., Salamati, R., Shafei, A., Solaymani, S., et al. (2006). Active transtension inside central Alborz: A new insight into northern Iran–southern Caspian geodynamics. *Geology*, 34, 477–480.
- Rizza, M., Vernant, P., Ritz, J. F., Peyret, M., Nazari, H., Nankali, H., et al. (2013). Morphotectonics and geodetic evidences for a constant slip-rate over the last 45 kyr along the Tabriz Fault (Iran). *Geophysical Journal International*, 193(3), 1083–1094.
- Scholz, C. (1988). The mechanism of seismic quiescence. *Pure and Applied Geophysics*, 126, 701–718.
- Scholz, C. (1990). *The mechanics of the earthquakes and faulting*. Cambridge University Press, ISBN: 0–521–33443–8.
- Sepahvand, M. R., Yamini-Fard, F., Tatar, M., & Abbassi, M. R. (2012). Aftershocks study of the 2006 Silakhr earthquake (Zagros, Iran): Seismological evidences for a pull-apart basin along the Main Recent Fault, Doroud segments. *Journal of Seismology*, 16(2), 233–251.
- Solaymani Azad, Sh, Nemati, M., Abbassi, M. R., Foroutan, M., Hesarani, Kh, Dominguez, S., et al. (2019). Active-couple indentation in geodynamics of NNW Iran: Evidence from synchronous left- and right-lateral co-linear seismogenic faults in western Alborz and Iranian Azerbaijan domains. *Tectonophysics*, 754, 1–17.
- Stuart W.D., and Aki K. (eds.) (1988). Intermediate-term earthquake prediction. *Pure Appl. Geophys.*, 126(2–4), 175–718.
- Talebian, M., & Jackson, J. A. (2002). Offset on the Main Recent Fault of NW Iran and implication for the late Cenozoic tectonics of the Arabia-Eurasia collision zone. *Geophysical Journal International*, 150, 422–439.
- Talebian, M., & Jackson, J. A. (2004). A reappraisal of earthquake focal mechanisms and active shortening in the Zagros mountains of Iran. *Geophysical Journal International*, 156, 506–526.
- Tatar, M., Hatzfeld, D., & Ghafory-Ashtiany, M. (2004). Tectonics of the Central Zagros (Iran) deduced from micro-earthquake seismicity. *Geophysical Journal International*, 156, 255–266.
- Tatar, M., Hatzfeld, D., Moradi, A., & Paul, A. (2005). The 2003 December 26 Bam earthquake (Iran), Mw 6.6, aftershock sequence. *Geophysical Journal International*, 163, 90–105. <https://doi.org/10.1111/j.1365-246X.2005.02639.x>.
- Tchalenko, J. S., Braud, J., & Berberian, M. (1974). Discovery of three earthquake faults in Iran. *Nature*, 248, 661–663.
- Vernant, P., Nilforoushan, F., Hatzfeld, D., Abassi, M., Vigny, C., Masson, F., et al. (2004). Contemporary crustal deformation and plate kinematics in Middle east constrained by GPS measurements in Iran and northern Oman. *Geophysical Journal International*, 157, 381–398.
- Walker, R. T., Bergman, E. A., Elliott, J. R., Fielding, E. J., Ghods, A. R., Qorashi, M., et al. (2013). The 2010–2011 South Rigan (Baluchestan) earthquake sequence and its implications for distributed deformation and earthquake hazard in southeast Iran. *Geophysical Journal International*, 193, 349–374.
- Walker, R. T., Bergman, E. A., Szeliga, W., & Fielding, E. J. (2011). Insights into the 1968–1997 Dasht-e-Bayaz and Zirkuh earthquake sequences, eastern Iran, from calibrated relocations, InSAR and high-resolution satellite imagery. *Geophysical Journal International*, 187(3), 1–27.
- Walker, R., & Jackson, J. (2004). Active tectonics and late Cenozoic strain distribution in central and eastern Iran. *Tectonics*, 23, 1–24.
- Walker, R., Jackson, J., & Baker, C. (2004). Active faulting and seismicity of the Dasht-e-Bayaz region, eastern Iran. *Geophysical Journal International*, 157, 265–282.
- Wells, D. L., & Coppersmith, K. J. (1994). New empirical relationship among magnitude, rupture length, rupture area and surface displacement. *Bulletin of the Seismological Society of America*, 84, 974–1002.
- Wessel, P., & Smith, W. H. F. (1998). New improved version of Generic Mapping Tools released. *EOS Transactions of the American Geophysical Union*, 79(47), 579.
- Wyss, M., & Habermann, R. E. (1988). Precursory seismic quiescence. *Pure and Applied Geophysics*, 126(2–4), 701–718.

- Yamini-Fard, F., Hatzfeld, D., Farahbod, A. M., Paul, A., & Mokhtari, M. (2007). The diffuse transition between the Zagros continental collision and the Makran oceanic subduction (Iran): Microearthquake seismicity and crustal structure. *Geophysical Journal International*, *170*, 182–194.
- Yamini-Fard, F., Hatzfeld, D., Tatar, M., & Mokhtari, M. (2006). Microearthquake seismicity at the intersection between the Kazerun Fault and the Main Recent Fault (Zagrs, Iran). *Geophysical Journal International*, *166*, 186–196.
- Yazdanfar, C., Nemati, M., Agh Ataby, M., Roustaei, M., & Nilfouroushan, F. (2018). Stress transfer, aftershocks distribution and InSAR analysis of the 2005 Dahuieh earthquake, SE Iran. *Journal of African Earth Science*, *147*, 211–219.